J. Fluid Mech. (1971), *vol.* 49, *part* 2, *pp.* 361–372
Printed in Great Britain

Instability and breakup of charged liquid jets

By A. L. HUEBNER AND H. N. CHU
Rocketdyne, a Division of North American Rockwell Corporation,
Canoga Park, California

(Received 8 December 1970)

Drops formed from the breakup of charged cylindrical liquid jets have been shown to be smaller than those formed in the unelectrified case. This change has been related to electrically induced instabilities on the jet. Small-perturbation analysis was used to formulate the Lagrangian and write the differential equation for the jet. Non-dimensionalized plots of the solutions exhibit the stabilizing or destabilizing influences of surface tension and electric effects, and allow these influences to be related back to liquid physical properties. Drop diameter to be expected from breakup of the electrified jet was calculated as a function of jet diameter, physical properties of the liquid, jet electrification, and the mode of instability dominating the breakup process.

Introduction

The effect of induced charges on liquid jets has been a subject of study for many years. Rayleigh (1878) analyzed the axisymmetrical instability of flowing jets and showed that they disintegrated into drops corresponding to the wavelength of fastest growth. Basset (1894) calculated the stability of axisymmetrical waves on conducting jets, including the effects of charge, velocity, viscosity, and ambient fluid. Schneider *et al.* (1967) extended Rayleigh's analysis by including the effect of electric charge and indicated that their result was in agreement with Basset's more comprehensive study. Recently, Taylor (1969) considered the lowest mode of instability which causes non-axisymmetric waves on the charged jet.

Limited experimental work has been accomplished with charged cylindrical jets. Magarvey & Outhouse (1962) examined the spectrum of instabilities exhibited by charged water jets but did not relate them to theory; they also made qualitative observations concerning the decrease in drop size resulting from the length-extension instability occurring at high electrification of the jet. Schneider *et al.* (1967) were concerned with producing uniform sized charged droplets from electrified water jets. Consequently, their investigation was limited to the axisymmetric mode of jet breakup, with droplet size controlled by an applied driving frequency. Huebner (1969, 1970) investigated the relationship of jet instabilities to jet diameter, jet flow rate, and liquid properties, and quantified the observed decrease in drop size with increasing jet electrification.

In this paper, previous analyses are extended to incorporate a description of non-axisymmetric instabilities of arbitrary wave-number, as well as the axisymmetric instability. The results are compared, in the appropriate limit, to

those reported previously. The relative influence of the surface tension and electrical terms is particularly emphasized.

This comprehensive analysis is applied to drop formation from electrified jets and is employed to suggest the manner in which electrification causes decreased drop size. Direct comparison of experimental and predicted drop sizes is not possible because the infinite cylindrical geometry assumed in the analytical model, and essential to the success of a general theoretical treatment, conflicts with the requirements of the experimental setup. The analysis thus represents a limiting case for comparison with experimental results, and provides a mechanism for considering the influence of geometry and applied potential on drop formation from electrified jets.

Theoretical analysis

The shapes of the two modes, $m = 0$ and $m = 1$, are sketched in figures 1 and 2, together with some of the nomenclature used. The surface of the perturbed cylinder is represented by the equation

$$r_0 = a_0 + c\cos m\theta \cos kz, \tag{1}$$

where c is proportional to $e^{\omega t}$ and a_0 is related to the original jet radius a by the requirement that the volume of liquid per wavelength $\lambda(= 2\pi/k)$ remains unchanged, i.e.

$$\frac{1}{\lambda}\int_0^{\lambda}\int_0^{2\pi} \tfrac{1}{2}r_0^2 d\theta\, dz = \pi a^2.$$

c, whose motion is to be studied, characterizes the infinitesimal deviation from the cylindrical shape, so that $(c/a) \ll 1$; m and k are the circumferential and longitudinal wave-numbers, respectively, and ω characterizes the growth rate of the wave.

Following Rayleigh and Schneider *et al.*, we develop the Lagrange equation of motion for the generalized co-ordinate c. It is assumed that the potential on the surface of the jet is constant at V_0 and that, concentric to the unperturbed jet and at a distance b from its axis, is a grounded cylindrical electrode. The potential in the region between the unperturbed jet and the electrode is given by

$$V_c = V_0 \frac{\ln(b/r)}{\ln(b/a)}. \tag{2}$$

There is an additional component of the potential, V_p, due to the perturbation. This component satisfies the Laplace equation $\nabla^2 V_p = 0$. Writing

$$V_p = R(r)\cos m\theta \cos kz,$$

it follows that

$$\frac{d^2R}{dr^2} + \frac{1}{r}\frac{dR}{dr} - \left(k^2 + \frac{m^2}{r^2}\right)R = 0.$$

Thus

$$R(r) = AI_m(kr) + BK_m(kr),$$

where I_m and K_m are the modified Bessel functions of the first kind and the second kind, respectively, both of integral order m.

Using the boundary condition $V_p = 0$ at $r = b$

$$B = -A\frac{I_m(kb)}{K_m(kb)}.$$

The potential in the region between the perturbed jet and the electrode is therefore given by

$$V = V_0\frac{\ln(b/r)}{\ln(b/a)} + A\left[I_m(kr) - \frac{I_m(kb)}{K_m(kb)}K_m(kr)\right]\cos m\theta\cos kz,$$

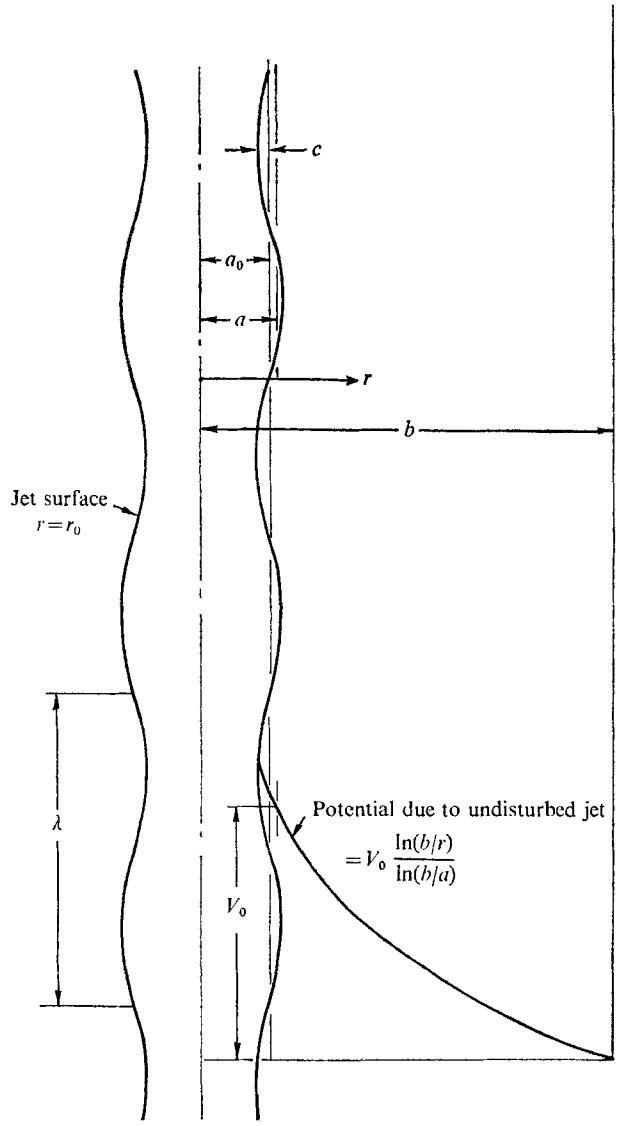

FIGURE 1. Axisymmetric mode of jet instability, circumferential wave-number $m = 0$.

where the constant A is to be determined from the boundary condition on the perturbed surface of the jet.

At

$$r = r_0 = a_0 + c\cos m\theta\cos kz \approx a(1 + (c/a)\cos m\theta\cos kz),\ V = V_0.$$

Hence

$$V_0 = \frac{V_0}{\ln(b/a)}\ln\left[\frac{b}{a}\left(1 - \frac{c}{a}\cos m\theta\cos kz\right)\right] + A\left[I_m(ka) - \frac{I_m(kb)}{K_m(kb)}K_m(ka)\right]\cos m\theta\cos kz.$$

Thus

$$V = V_0\frac{\ln(b/r)}{\ln(b/a)} + \frac{V_0(c/a)}{\ln(b/a)}\frac{K_m(kb)\,I_m(kr) - I_m(kb)\,K_m(kr)}{K_m(kb)\,I_m(ka) - I_m(kb)\,K_m(ka)}\cos m\theta\cos kz. \qquad (3)$$

This expression is correct up to first order in (c/a).

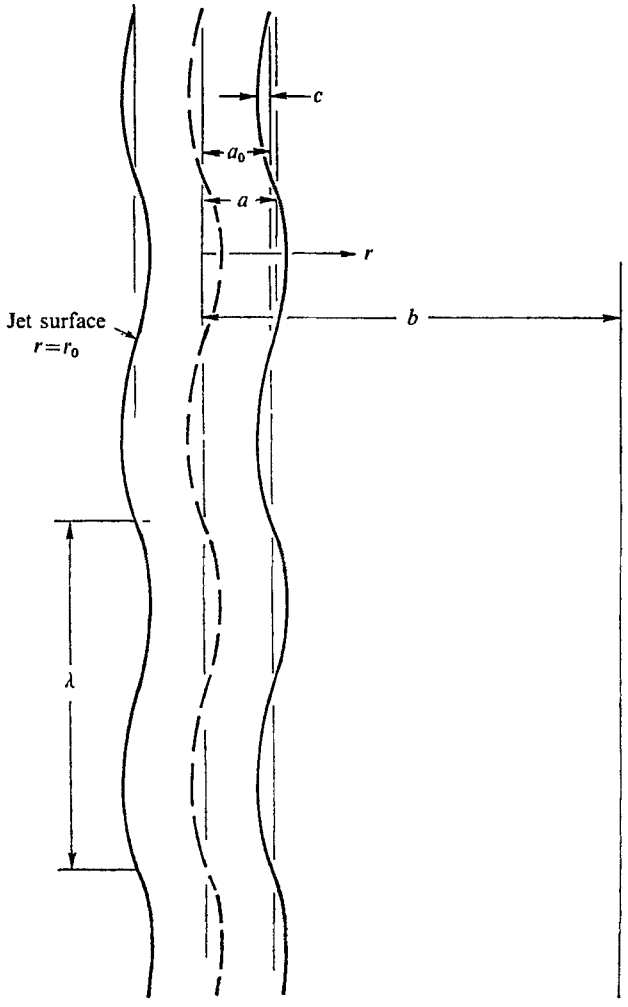

FIGURE 2. Lowest-order non-axisymmetric mode of jet instability, circumferential wave-number $m = 1$.

The potential energy of the jet due to electrification is

$$P_L = \tfrac{1}{2}V_0 \int \sigma \, dS$$

and the surface charge density is calculated from

$$\begin{aligned}\sigma &= -\epsilon_0(\mathbf{n}.\operatorname{grad} V)_{r_0} = -\epsilon_0 \left.\frac{\partial V}{\partial r}\right|_{r_0} \\ &= \frac{\epsilon_0 V_0}{a \ln(b/a)}\left[1 - \frac{c}{a}(1+kaI)\cos m\theta \cos kz\right],\end{aligned}$$

where

$$I = \frac{K_m(kb)\, I'_m(ka) - I_m(kb)\, K'_m(ka)}{K_m(kb)\, I_m(ka) - I_m(kb)\, K_m(ka)}$$

and ϵ_0 is the permittivity of free space. Also

$$\begin{aligned}dS &= \left[1 + \left(\frac{1}{r_0}\frac{\partial r_0}{\partial \theta}\right)^2 + \left(\frac{\partial r_0}{\partial z}\right)^2\right]^{\frac{1}{2}} r_0 \, d\theta \, dz \\ &= a[1 + (c/a)\cos m\theta \cos kz]\, d\theta \, dz \\ &= r_0 \, d\theta \, dz.\end{aligned}$$

Hence

$$P_L = \frac{\pi \epsilon_0 V_0^2}{\ln(b/a)}\left[1 - \frac{1}{4}\left(\frac{c}{a}\right)^2 (1+kaI)\,(1+\delta_{0,m})\right],$$

where $\delta_{0,m} = 1$ for $m = 0$, and $\delta_{0,m} = 0$ otherwise. The potential energy of the unperturbed cylinder is

$$P_0 = \tfrac{1}{2} Q_{CL} V_0 = \frac{\pi \epsilon_0 V_0^2}{\ln(b/a)},$$

where $Q_{CL} = 2\pi\epsilon_0 V_0 / \ln(b/a)$ is the charge per unit length of the unperturbed cylinder. Therefore

$$P_R^* = -\frac{\pi}{4}\frac{\epsilon_0 V_0^2}{\ln(b/a)}\left(\frac{c}{a}\right)^2 (1+kaI)\,(1+\delta_{0,m})$$

represents the electrical energy change of the jet above, without considering that of the charging system. The latter is $(-2P_R^*)$ so that the total change in electrical energy is $P_R = -P_R^*$. The change in the potential energy due to surface tension, P_T, and the kinetic energy, K, have already been given by Chandrasekhar (1961). They are, per unit length

$$P_T = \frac{\pi}{4} T \frac{c^2}{a}(k^2a^2 + m^2 - 1)\,(1+\delta_{0,m})$$

and

$$K = \frac{\pi}{4}\frac{\rho a^2}{ka}\frac{I_m(ka)}{I'_m(ka)}(1+\delta_{0,m})\,\dot{c}^2,$$

where T is surface tension and ρ is liquid density.

Using the Lagrangian $L = K - P_T - P_R$ in the Lagrangian equation yields

$$\ddot{c} - \frac{T}{\rho a^3}\left[\frac{(1-m^2-k^2a^2)\,(ka)\,I'_m(ka)}{I_m(ka)}\right] c + \frac{\epsilon_0 V_0^2 (ka)\, I'_m(ka)}{\rho a^4 \ln(b/a)\, I_m(ka)}[1+kaI]\, c = 0.$$

With $c \sim e^{\omega t}$

$$\omega^2 = \frac{T}{\rho a^3}\left[\frac{(1-m^2-k^2a^2)\,(ka)\,I'_m(ka)}{I_m(ka)}\right] - \frac{\epsilon_0 V_0^2(ka) I'_m(ka)}{\rho a^4 \ln(b/a)\, I_m(ka)}\left[1 + ka\frac{K'_m(ka)}{K_m(ka)}\right], \quad (4)$$

using $I \approx K'_m(ka)/K_m(ka)$ for large b/a. This can be written in the non-dimensional form

$$\frac{\omega^2}{T/\rho a^3} = \frac{kaI'_m(ka)}{I_m(ka)}\left[(1-m^2-k^2a^2) - \Gamma\left(1 + ka\frac{K'_m(ka)}{K_m(ka)}\right)\right], \quad (5)$$

with

$$\Gamma = \frac{\epsilon_0 V_0^2}{\rho a^4 \ln(b/a)} \Big/ \frac{T}{\rho a^3} = \frac{\epsilon_0 V_0^2}{Ta \ln(b/a)}.$$

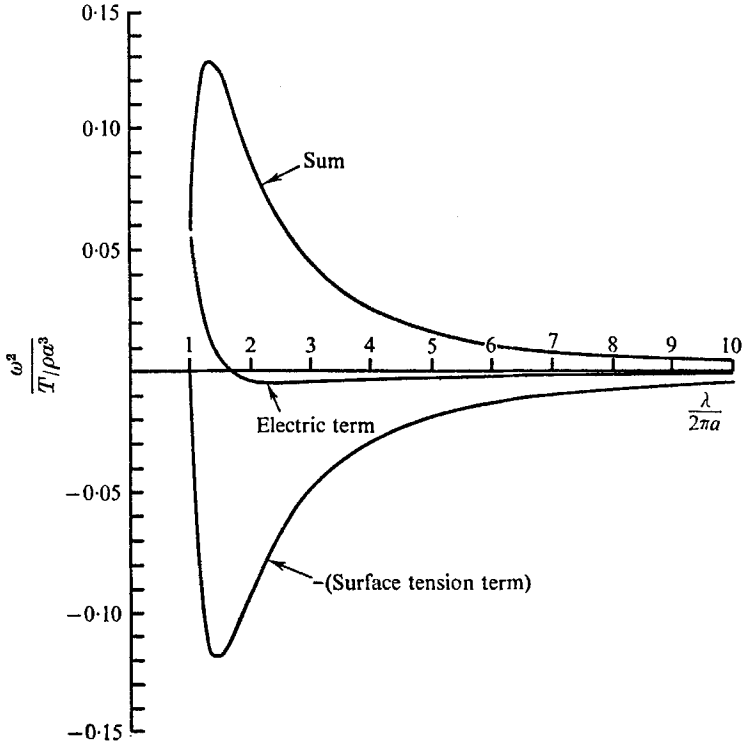

FIGURE 3. Stability diagram for an electrified cylindrical liquid jet with $m = 0$. The parameter measuring the ratio of electrical influence to surface tension influence on instability, $\Gamma = 0{\cdot}3$. Positive $\omega^2/(T/\rho a^3)$ represents wave growth and negative $\omega^2/(T/\rho a^3)$ represents oscillatory motion.

The dispersion relationship (4) reduces to

$$\omega^2 = \frac{T}{\rho a^3}\frac{(1-k^2a^2)\,(ka)\,I_1(ka)}{I_0(ka)} - \frac{\epsilon_0 V_0^2(ka)\, I_1(ka)}{\rho a^4 \ln(b/a)\, I_0(ka)}\left[1 - ka\frac{K_1(ka)}{K_0(ka)}\right] \quad (6)$$

for $m = 0$ and using $I'_0(ka) = I_1(ka)$, $K'_0(ka) = -K_1(ka)$. Equation (6) agrees with the result obtained by Schneider *et al.*, and with the earlier result of Basset as corrected recently by Taylor. (Basset's original result is not dimensionally

correct; the change introduced by Taylor rectifies this error.) Writing the dispersion relationship for the case $m = 1$ yields

$$\omega^2 = -\frac{T}{\rho a^3}\frac{k^3a^3 I_1'(ka)}{I_1(ka)} - \frac{e_0 V_0^2(ka)\, I_1'(ka)}{\rho a^4 \ln(b/a)\, I_1(ka)}\left[1 + ka\frac{K_1'(ka)}{K_1(ka)}\right], \tag{7}$$

which is in agreement with the result obtained by Taylor for this case.

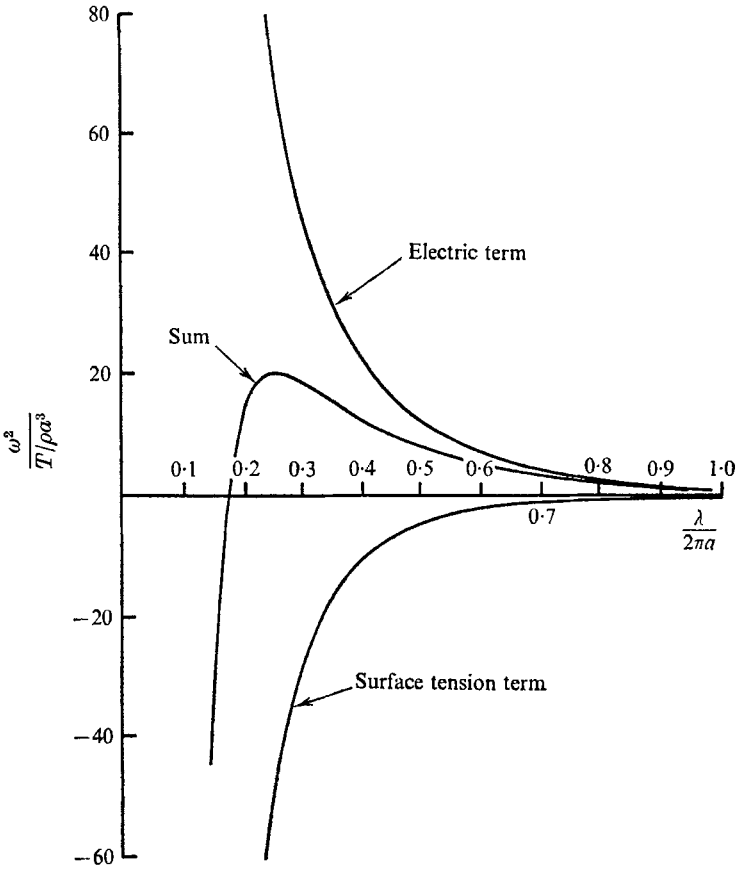

FIGURE 4. Stability diagram for an electrified cylindrical liquid jet ($m = 0$, $\Gamma = 6$).

Numerical results obtained from equation (5) for the axisymmetric mode $m = 0$ and for two values of Γ are shown on figures 3 and 4; these values of Γ correspond to very slight and to moderate electrification, respectively. The electrical and surface tension terms are plotted separately, as well as the sum of the two, for convenience in analyzing the relative influence of the two terms. Similar results for the kink mode $m = 1$ are shown on figures 5 and 6. Positive ω^2 represents wave growth and negative ω^2 represents oscillatory motion; therefore, the part of the curve lying above the abscissa represents instability, and that lying below the abscissa represents stability. The exception is the curve

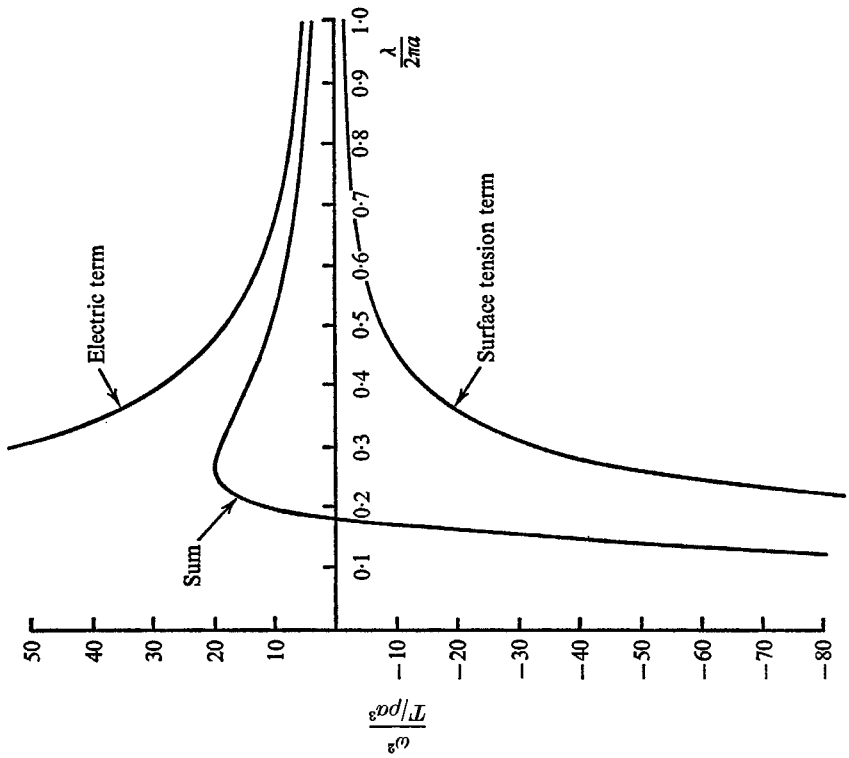

FIGURE 6. Stability diagram for an electrified cylindrical liquid jet ($m = 1, \Gamma = 6$).

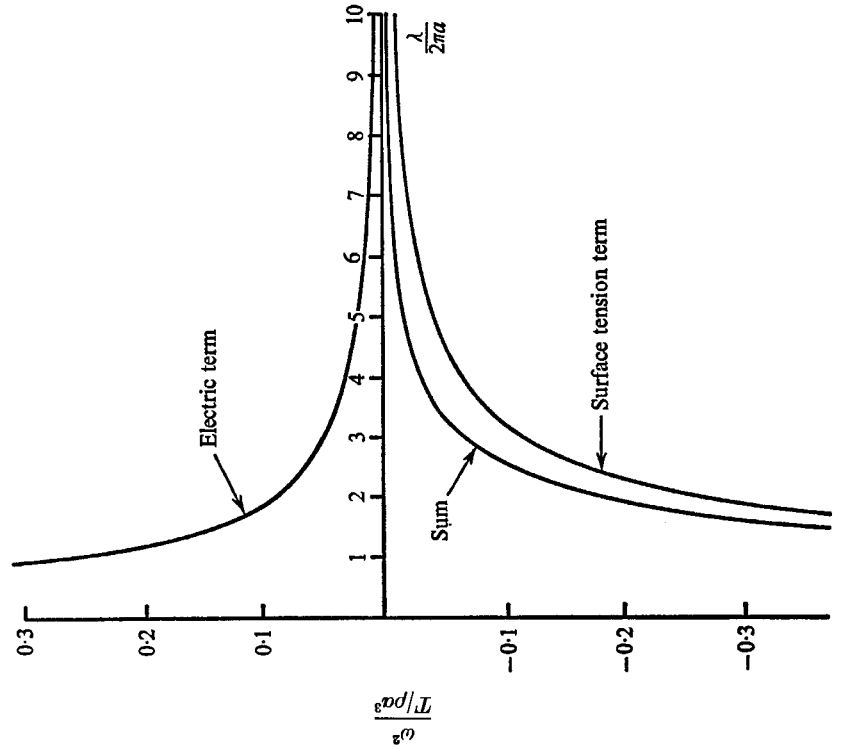

FIGURE 5. Stability diagram for an electrified cylindrical liquid jet ($m = 1, \Gamma = 0{\cdot}3$).

representing surface tension on figure 3, which was plotted inverted so that it could be distinguished from the sum curve.

The way in which the electrical charge causes a reduction in drop size is made clear by comparing figures 3 and 4, and also figures 5 and 6. In figure 3, for example, although the electrical charge stabilizes the jet slightly for $\lambda/2\pi a > 1{\cdot}66$, it destabilizes the jet substantially for $\lambda/2\pi a < 1{\cdot}66$. The effect is to shift the maximum from about $\lambda/2\pi a = 1{\cdot}4$, the well-known result for an uncharged jet,

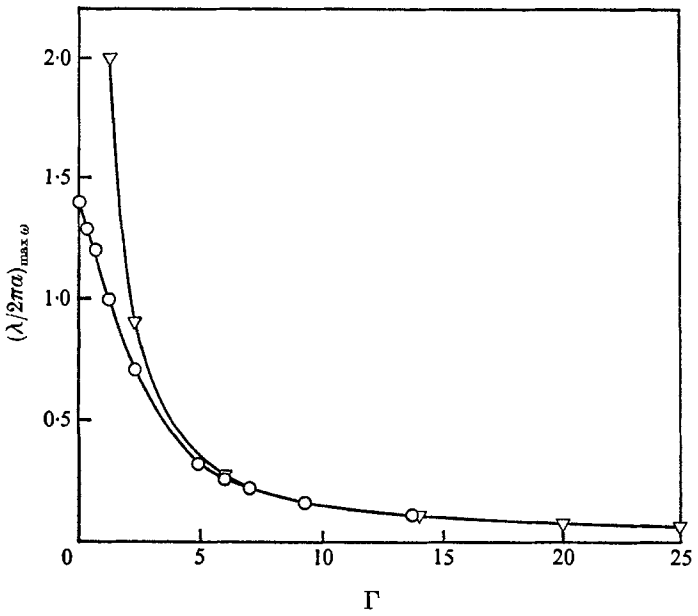

FIGURE 7. Variation of longitudinal wavelength of the jet instability, at maximum growth rate, with electrification for: ○, $m = 0$; and ▽, $m = 1$.

down slightly to about 1·3, with an attendant slight increase in the non-dimensional growth rate, $\omega^2/(T/\rho a^3)$, from 0·12 to 0·13. The trend continues with increasing values of Γ as indicated on figure 4 and in the summary of calculated results for $m = 0$ presented on figure 7. Before the stabilizing influence of the electric charge can be realized at longer wavelengths, the jet becomes destabilized at shorter wavelengths. Moreover, the phenomenon is more pronounced the higher the charge.

For the $m = 0$ mode, the effect of surface tension is stabilizing for $\lambda/2\pi a < 1$ and destabilizing for $\lambda/2\pi a > 1$, whereas the effect of electric charge is stabilizing for $\lambda/2\pi a > 1{\cdot}66$ and destabilizing for $\lambda/2\pi a < 1{\cdot}66$. For the $m = 1$ mode there are no such cut-off wavelengths. Surface tension stabilizes and electric charge destabilizes the jet, as indicated on figures 5 and 6. The magnitude of the electrification in figure 5 is quite small, so that surface tension dominates at all wavelengths and the jet is stable. With increasing jet electrification, the increased influence of the electric term destabilizes the jet more and more pronouncedly, as indicated on figures 6 and 7. At moderate jet electrification there is no

pronounced wavelength of fastest growth (figure 6), but the curve representing the sum of the electric and surface tension effects develops a more pronounced maximum with increasing jet electrification.

Drop formation from charged jets

Rayleigh calculated for the growth constant of an unelectrified cylindrical jet

$$\omega^2 = \frac{T}{\rho a^3}\frac{kaI_0'(ka)}{I_0(ka)}(1-k^2a^2) = \frac{T}{\rho a^3}f(ka).$$

This is the limiting form of equation (4) when the jet is not electrified. The function $f(ka)$ presents a maximum for $ka = 2\pi a/\lambda = \pi/4{\cdot}51$, or $\lambda/2\pi a = 1{\cdot}4$, cited earlier; the wavelength of the fastest growing perturbation is thus $\lambda = 4{\cdot}51 \times 2a$. Dabora (1967) has shown further that the diameter d of the drops most likely to be formed by jet breakup, where the drop mass is considered equivalent to that of a one-wavelength-long cylinder of the jet, is given by the well-known result $d = 1{\cdot}89 \times 2a$.

This procedure for calculating drop sizes gives a particularly simple result because both m and Γ vanish. When one or both of these does not vanish, the calculation is modified as follows. Following Dabora, the drop mass, $\pi\rho d^3/6$, is equated to that of a one-wavelength-long cylinder, $\pi\rho a^2\lambda$. Rearrangement gives for the diameter of the drops formed from the wavelength of most rapid growth

$$d = (12\pi)^{\frac{1}{3}}\left(\frac{\lambda}{2\pi a}\right)^{\frac{1}{3}}_{\max\omega} a. \tag{8}$$

The value of $(\lambda/2\pi a)^{\frac{1}{3}}_{\max\omega}$ for given electrical conditions, liquid properties, and jet radius, is determined for the appropriate mode from a plot such as that of figure 7.

Discussion

The range of values of Γ shown on figure 7 lies within the range of values employed experimentally (Huebner 1969, 1970). (Applied potential was varied from 0 to 25 kV, while a and the ratio b/a were varied by about a factor of 10.) The anomalously large drops associated with the $m = 1$ mode for small Γ are not observed (the $m = 1$ mode itself is not observed) because the growth rate of the $m = 0$ mode is larger. The wavelength and drop size associated with $m = 0$ and $m = 1$ become equal at about the same value of Γ for which the growth rate of the $m = 1$ mode crosses over that for the $m = 0$ mode. The values of $(\lambda/2\pi a)_{\max\omega}$ on figure 7 for the $m = 0$ mode are therefore appropriate for use in calculating drop size from equation (8), even when the actual mode of jet disintegration is the kink mode $m = 1$.

The ratio of drop diameter to jet diameter calculated in this way for the $m = 0$ and $m = 1$ modes is shown as a function of the electrification parameter Γ on figure 8. These calculated values represent the limiting case of drop size reduction produced by electrification of the jet, assuming the instability leading to jet

breakup to be of the type considered in the theoretical model. That is, instabilities in which the wall of the jet ruptures or jet surface-growth occurs are not limited to drop size reductions consistent with the calculated curve and will, in general, yield smaller drop sizes, as observed by Magarvey & Outhouse (1962) and Huebner (1969, 1970). Recognizing this restriction, the calculated values of d/d_j represent

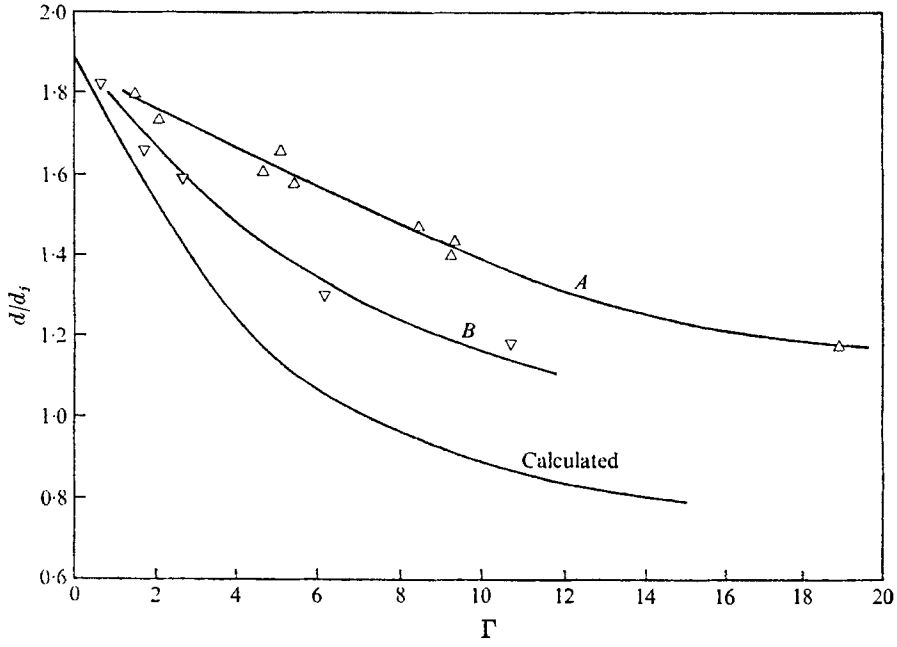

FIGURE 8. Calculated and experimental drop size variation with electrification for $m = 0$ and $m = 1$.

the limiting case of drop size reduction, for a given value of Γ, because electric potential is applied with maximum efficiency when the infinite cylindrical geometry assumed in the theory is applicable. Experimentally, of course, this is not the case. In our earlier experiments, for example, the geometry of the liquid collector was determined by the requirements that all drops be collected and that there be visual and photographic observation of jet breakup and drop dynamics. The result was a collector that conformed to the subsequently developed theoretical model relatively poorly. A plot of data obtained with this collector is shown as curve *A* of figure 8. The data points defining the plotted curve were obtained from experiments conducted with three jet diameters and two liquids, distilled water and isopropyl alcohol. These experimental data lie substantially above the calculated curve, consistent with the preceding remarks. Nevertheless, decrease in drop diameter of 25 per cent or more is achievable at reasonable applied potential.

After completion of the theoretical analysis, a new collector was constructed having approximately the same length but one-half the diameter of the previous collector so that the relative influence of the sides of the collector were increased with respect to the bottom. Failure to collect drops could be completely avoided

by limiting the potential applied to the jet to values below those at which surface-growth instabilities occur. Slits still had to be cut in the collector for observation of the jet distintegration and drop formation, but these were kept quite narrow. Great care was taken to minimize edge effects at the open end of the collector during test. Thus, this second collector was designed and used to obtain a closer approximation to the theoretical model, but, for purposes of experimental convenience, it was not attempted to duplicate the theoretical model as closely as possible. Data obtained with this collector using jets of distilled water are presented as curve B on figure 8. The approach to the calculated curve is considerably better than with the original collector, but the data still lie above the theoretical predictions, as expected.

Although the decrease in drop size indicated by the experimental curves on figure 8 is substantial, even closer approach to the calculated result is possible in many applications. In combustion applications, for example, slits in the collector are not required and there is no need to collect drops. Only edge effects remain to decrease the effectiveness of the applied potential, and these can be made quite small. With this relaxation of restrictions, the geometry (e.g. the ratio b/a) may be chosen to obtain drop size decreases equivalent to those plotted on figure 8 at lower applied potentials than those required for the experimental data cited.

This research was sponsored by the Office of Naval Research under Contract N00014-67-C-0474, Contract Identification no. NR094-348.

REFERENCES

BASSET, A. B. 1894 *Am. J. Math.* **16**, 13.

CHANDRASEKHAR, S. 1961 *Hydrodynamic and Hydromagnetic Stability.* Clarendon.

DABORA, E. K. 1967 *Rev. Sci. Instrum.* **38**, 502.

HUEBNER, A. L. 1969 *J. Fluid Mech.* **38**, 679.

HUEBNER, A. L. 1970 *Science, N.Y.* **168**, 118.

MAGARVEY, R. H. & OUTHOUSE, L. E. 1962 *J. Fluid Mech.* **13**, 151.

RAYLEIGH, LORD 1878 *Proc. London Math. Soc.* **10**, 4.

SCHNEIDER, J. M., LINDBLAD, N. R., HENDRICKS, C. E. & CROWLEY, J. M. 1967 *J. Appl. Phys.* **38**, 2599.

TAYLOR, G. I. 1969 *Proc. Roy. Soc.* A **313**, 453.